PROCESSING CONDITIONS AND REDUCTION OF OXIDES DURING SINTERING OF CHROMIUM PRE-ALLOYED STEEL

M. Hrubovčáková, E. Dudrová, E. Hryha, M. Kabátová

Abstract

Oxide reduction processes and their temperature intervals during sintering of Fe-3Cr-0.5Mo pre-alloyed powder have been identified using continuous monitoring of processing gas composition (CO, CO_2, H_2O). Their interpretation is in relation to density (6.5-7.4 $g \cdot cm^{-3}$), sintering temperature (1120 and 1200°C), heating and cooling rates (10 and 50°C/min), carbon addition (0.5/0.6/0.8%), and type of sintering atmosphere (10%H_2-N_2, N_2), respectively. The progress in reduction processes was evaluated by the relative change in oxygen and carbon contents and related to resultant fracture strength. Higher sintering temperature (1200°C) and low density (6.5 $g \cdot cm^{-3}$) result in a relative decrease of oxygen content by more than 80%. Higher cooling rate (50°C/min) eliminates re-oxidation during cooling. The reducing ability of the nitrogen atmosphere can be improved by sintering in a graphite container. High density of 7.4 $g \cdot cm^{-3}$, achieved by a pressing/re-pressing method, causes a slowing down of the reduction processes. In terms of optimizing strength, the carbon content in this sintered steel should not be higher than ~0.45%.

Keywords: chromium pre-alloyed steel, sintering, oxide reduction, processing gas composition

INTRODUCTION

Despite longstanding intensive research resulting in the development of different variants of pre-mixed alloys, there was no real industrial use of cheap alloying elements, such as Cr, Mn and Si. Hence production of water atomized chromium pre-alloyed powders (e.g. Astaloy CrM, Astaloy CrL) has brought a fundamental change, consisting in the decrease of the oxidation activity of chromium in solid solution. Chromium pre-alloyed powders, due to the excellent hardenability of Fe-Cr-C system, have an outstanding predisposition for production of highly stressed sintered structural components [1-7]. Full utilization of all advantages of Cr-alloying requires perfect oxide purity of interfaces, which also strongly relates to the reduction of oxides created on powder particle surfaces - already in the stage of powder production [8-14]. Consistent solution of this problem can contribute to lowering of the differences between the strength properties of wrought and sintered chromium- alloyed steels.

Reduction/oxidation processes in a powder compact during sintering are controlled by a variety of factors, such as sintering temperature, heating and cooling rates, protective atmosphere used, carbon content and density. In general, the required reduction conditions during sintering of metal compacts are designed by thermodynamical stability of oxides or

Monika Hrubovčáková, Eva Dudrová, Margita Kabátová, Institute of Materials Research, Slovak Academy of Sciences, Košice, Slovak Republic
Eduard Hryha, Chalmers University of Technology, Göteborg, Sweden

their reducibility by H_2, or through carbothermal reactions. Depending on processing conditions and on-going chemical reactions, the composition of processing gas alters during sintering [10-17].

Mitchell and Cias [11] reported the necessary reduction sintering conditions obtained through thermodynamical calculations of maximum tolerable partial pressure of CO, CO_2, H_2O in the processing gas. Originating knowledge of chemical interactions during the sintering of Cr-alloyed steels was reported by Danninger et al. [16-20], Ortiz and Castro [10, 21] and Hryha et al. [9, 12-14, 21-26]. Investigations have shown that, for a porous powder compact, there is a need to respect the fact that the chemical reactions between applied sintering atmosphere and the external compact surface may be quite different than those taking place in inner pores, called "micro-climate" [11]. In the case of powder steels alloyed with elements having high oxidation affinity, special attention should be paid to the evolution of reduction/oxidation processes during the critical stage of sintering, which is the heating stage [14, 24, 26].

This contribution deals with the study of the effect of sintering parameters (temperature, sintering atmosphere composition, heating and cooling rates), carbon content and density on reduction processes during the sintering of Fe-3%Cr-0.5%Mo (Astaloy CrM) powder using continuous monitoring and analysis of processing gas composition over the whole sintering cycle. The progress of oxide reduction processes has been evaluated by oxygen and carbon contents and related to fracture strength values resulting from sintering.

EXPERIMENTAL MATERIAL AND METHODS

The investigated material was water atomized Fe–3%Cr-0.5%Mo (Astaloy CrM) powder (Höganäs AB, Sweden) with O_2 content in as-received state of 0.197%. The carbon in the form of Kropfmühl UF4 graphite was admixed in the amount of 0.5, 0.6 and 0.8 wt.%. Homogenized powder mixes were compacted into cylindrical compacts Ø10x12 mm^3 with the density of 6.5, 6.8, and 7.1 $g \cdot cm^{-3}$, respectively. By the double-pressing procedure, consisting of a compaction at 800 MPa, annealing at 750°C/30 min in 10%H_2-N_2 (purity 5.0) and re-pressing at 800 MPa, cylindrical compacts with the density of 7.4 $g \cdot cm^{-3}$ were also prepared. Sintering was carried out in a laboratory furnace Aneta 1 at 1120 and 1200ºC for 30 min. Two different heating and cooling rates, 10 and 50ºC/min were applied. The sintering furnace is a part of the set-up for processing gas composition monitoring, Fig.1, originally installed at the IMR SAS laboratory [26]. The set-up arrangement allows analyzing in-line the CO, CO_2, H_2O contents in the processing gas during the whole sintering cycle. The atmosphere used was a mixture of 10%H_2-N_2 (purity of 5.0 and 6.0) and N_2 (purity of 5.0). Moreover, these atmospheres were purified by drying with liquid nitrogen. Therefore the inlet dew point (monitored by the SHAW Super-Dew Hydrometer) was ~ -68°C. The flow-rate of the atmosphere was always 2 l/min. In each experiment six identical samples were kept in an open ferritic stainless steel container from which the processing gas was continually sampled using a ferritic stainless steel tube, Fig.1. The dew point (H_2O content) was monitored by Michell Cermet II sensor, CO and CO_2 contents by non-disperse infrared analysers on the base of Gas Card II Plus sensor. All sensors were connected to a computer and continuous recording of the CO, CO_2, and H_2O contents was performed by special software. Microstructure was observed using light (Olympus GX 71) and scanning electron microscopy (Jeol JSM 7000F equipped with INCA EDX analyzer). Oxygen and carbon contents in the sintered material were analyzed using LECO TC36 Instrument. The fracture strength, R_{FR}, was evaluated by non-standard "button" tensile test method [26, 27]; the button-shaped samples were machined from sintered cylinders.

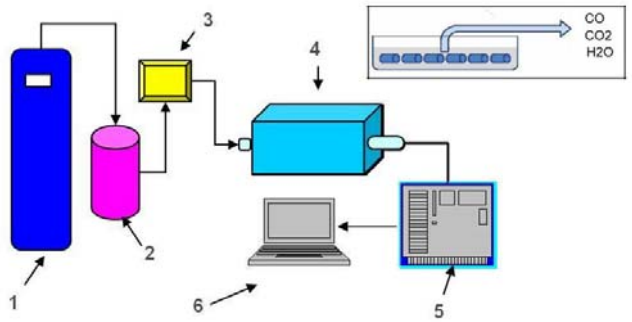

1-gas micture (H2-N2), 2- liquid nitrogen drayer, 3-hygrolog (inlet dew point),
4-furnance (ANETA-1), 2-CO, CO2, H2O analyzers, 6-PC

Fig.1. Scheme of sintering and processing gas composition monitoring set-up and steel container with the tube for gas sampling.

RESULTS AND DISCUSSION

Effect of density and sintering temperature on oxide reduction

The Astaloy CrM+0.5%C compacts with densities of 6.5, 6.8, 7.1, 7.4 g·cm^{-3} were heated to the temperatures of 730, 1120, 1200°C for 3 min and isothermally sintered at 1120 and 1200°C for 30 min. Sintering atmosphere was 10%H_2-N_2; heating rate was 10°C/min and cooling rate 50°C/min.

In Figures 2a-d are the records of the processing gas composition for all the tested densities and sintering temperature of 1200°C. The curves of H_2O, CO_2 and CO contents give information concerning chemical reactions and their temperature intervals during sintering.

Other useful information on reduction process provide O_2 and C contents, and fracture strengths obtained; these data are in Table 1.

The first H_2O peak linked with removing physically bonded water occurs at temperature of 180-195°C, depending on density. The reduction of continuous layer of surface less stable Fe_2O_3 oxide by H_2 starts at ~300°C and, depending on density, it reaches a maximum at 450-513°C. Direct carbothermal reduction connected with CO formation starts at ~750°C. The first, relatively small, peak on the CO profile, connected with surface iron oxides reduction by graphite in Fe-C contacts, occurs at 802, 820, 836 and 840°C, while increasing the temperature of the peak corresponds to the increasing density of compacts. Over the temperature of ~900°C the CO content rapidly increases. The CO peaks at 1081°C for 6.5g.cm^{-3} and at 1120°C for 6.8 g·cm^{-3} correspond to carbothermal reduction of stable surface Fe-Cr-Mn-Si oxides and iron oxides from internal pores communicating with the compact surface. At higher densities, of 7.1 and 7.4 g·cm^{-3} (when the reduction of oxides inside the compact becomes more difficult), the peak at ~ 1120°C has not been recorded, but in contrast, an increasing CO_2 content was indicated.

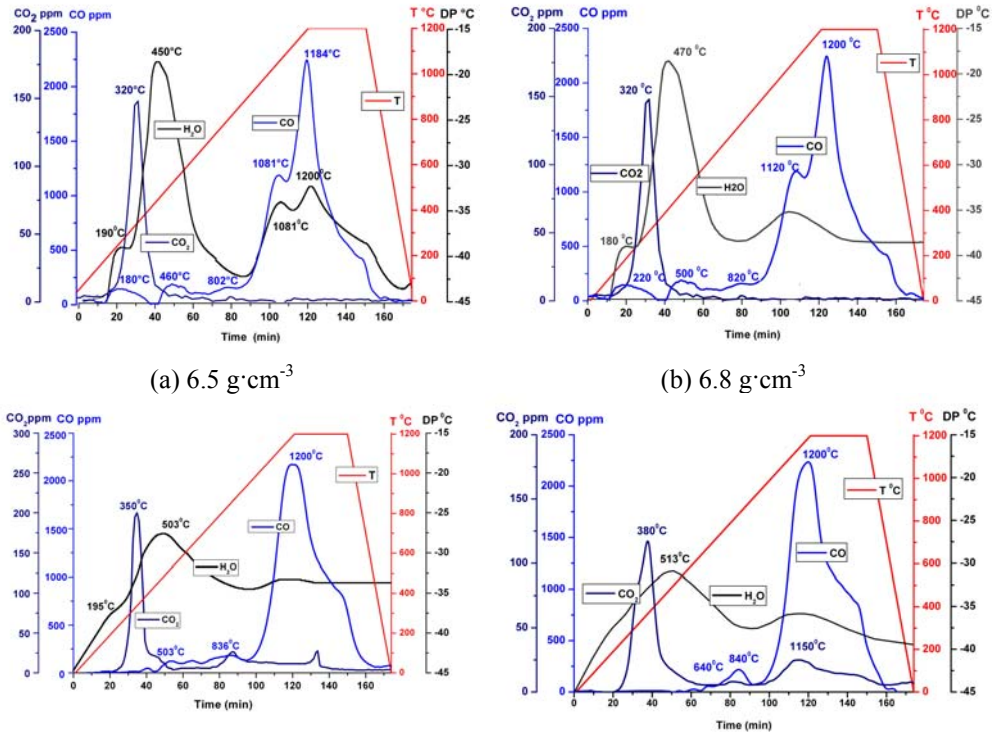

(a) 6.5 g·cm^{-3} (b) 6.8 g·cm^{-3}

(c) 7.1 g·cm^{-3} (d) 7.4 g·cm^{-3}

Fig.2. Records of processing gas composition during the sintering at 1200°C of Astaloy CrM + 0.5% C compacts with density of 6.5, 6.8, 7.1 and 7.4 g·cm^{-3}, respectively.

Tab.1. O_2 and C contents and R_{FR} resulting from heating and isothermal sintering of Ast CrM + 0.5% C.

Heating stage					Isothermal stage				
Density [g·cm^{-3}]	Temp. [°C]	O_2 [%]	C [%]	R_{FR} [MPa]	Density [g·cm^{-3}]	Temp. [°C]	O_2 [%]	C [%]	R_{FR} [MPa]
6.5	730	0.199	0.48	-	6.5	-	-	-	-
	1120	0.124	0.40	557		1120	0.098	0.42	562
	1200	0.069	0.36	752		1200	0.025	0.36	838
6.8	730	0.209	0.48	-	6.8	1120	0.097	0.42	754
	1120	0.144	0.44	693		1200	0.027	0.37	954
	1200	0.092	0.38	731		1120	0.133	0.43	929
7.1	730	0.214	0.48	-	7.1	1200	0.068	0.39	966
	1120	0.167	0.45	704		1120	0.156	0.45	416
	1200	0.136	0.40	954		1200	0.151	0.41	612

The observations are in good agreement with the results reported by Danninger et al. [17-19] and Chasoglou and Hryha [23]. The CO_2 peak linked with the decomposition of the carbonates and hydrocarbonates, present on the powder surface [14], occurs at 320°C

for densities of 6.5 and 6.8 g·cm^{-3}. For densities of 7.1 and 7.4 g·cm^{-3} this CO_2 peak is shifted to 350 and 380°C, a small CO_2 peak at ~1120°C at density of 7.4 g·cm^{-3} has been also recorded.

Analyzing the changes in oxygen and carbon contents, Table 1, indicates a small increase in oxygen content during heating to 730°C, by 0.016 and 0.003% at densities of 6.5 and 6.8 g·cm^{-3}. This is due to re-oxidation during the cooling stage, as also confirmed by weight gain of 1.02 and 6.09%. Heating to 1120°C resulted in decreasing oxygen content, by 15-37% for all densities, with lower values for higher densities. The same trend in oxygen content decrease, by 31-65%, was also observed during heating to 1200°C.

During the whole isothermal sintering cycle at 1120 and 1200°C, a further decrease in oxygen content was recorded, with an obvious positive effect of higher sintering temperature. It is important to note that at densities of 7.1 and 7.4 g·cm^{-3}, the oxygen content is higher for both sintering temperatures in comparison with densities of 6.5 and 6.8 g·cm^{-3}.

The oxygen content achieved for density of 6.5 g·cm^{-3} and sintering at 1120°C was 0.098%, and at 1200°C of ~0.025%, but for density of 7.4 g·cm^{-3} it was 0.156% for sintering at 1120°C and 0.151% for sintering at 1200°C. Similar trend in the change of C-content with increasing density is seen for both heating and isothermal sintering, Table 1.

Progress in reduction processes is also reflected on R_{FR} values, Table 1. Increasing the density from 6.5 to 7.1 g·cm^{-3} and heating temperature to 1200°C results in an increase of R_{FR} from 557 to 954 MPa. For isothermal sintering at 1120 and 1200°C, R_{FR} continually increases up to density of 7.1 g·cm^{-3}, when it reaches 929 MPa for 1120°C and 966 MPa for 1200°C. In accordance with a higher oxygen content for density of 7.4 g·cm^{-3}, due to weaker reduction processes, the fracture strength decreases to 416 and 612 MPa. The much lower values obtained for high density can be also explained by oxide transformation during the annealing step before re-pressing, as was shown by Hryha et al. [22].

Figures 3a, 4a show examples of the positive effect a higher sintering temperature on lowering oxide contamination for material density of 6.8 g·cm^{-3}. After sintering at 1120°C, at oxygen content of 0.097%, there exist small oxide particles forming a discontinuous network located particularly along original particle surfaces. By increasing the sintering temperature to 1200°C, a decrease in oxygen content to 0.027% results in a marked decrease of the amount of oxide particles, Fig.4a. A slight decrease in the C-content at sintering temperature of 1200°C has no significant influence on the bainitic microstructure, Figs.3b, 4b. Eventually only a presence of a small amount of pro-eutectoid carbides, Fig.3b [28, 29], may be expected. The failure, which occurred mainly along the surfaces of bainite packets, has a ductile character with fine shallow dimples, Figs.3c, 4c. Larger shallow dimples are initiated by small oxide particles. As a result of a higher oxidic purity and a favourable change in the shape of the pores, an increase of the fracture strength from 754 MPa for sintering at 1120°C to 954 MPa at 1200°C is observed.

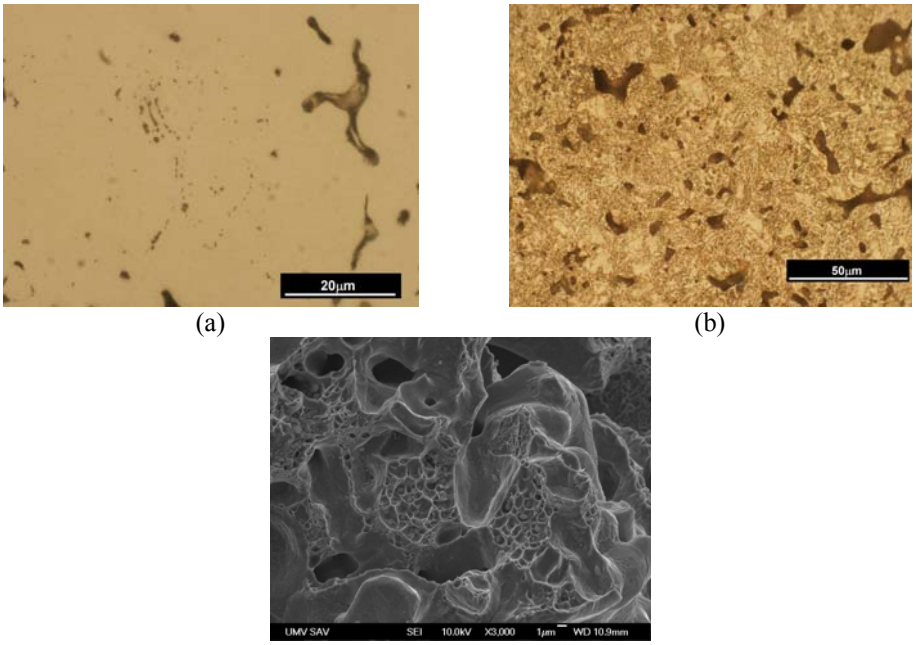

(a) (b)

(c)

Fig.3. Microstructure and fracture surface of the Fe-3Cr-0.5Mo-0.5C alloy with a density of 6.8 g·cm^{-3}, sintered at 1120°C for 30 min in 10%H_2-N_2 atmosphere. O_2=0.097%, C=0.42%.

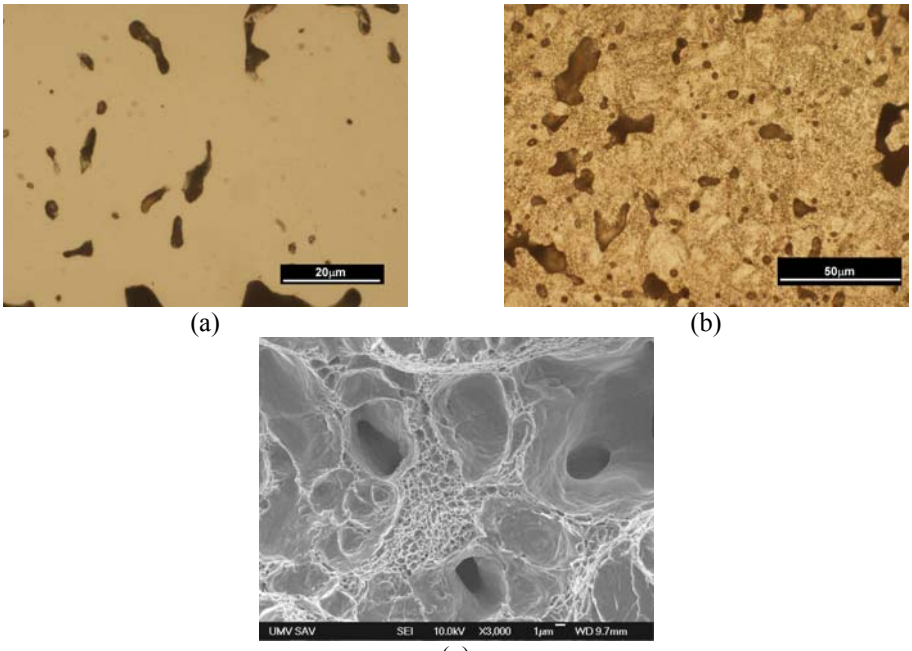

(a) (b)

(c)

Fig.4. Microstructure and fracture surface of the Fe-3Cr-0.5Mo-0.5C alloy with a density of 6.8 g·cm^{-3}, sintered at 1200°C for 30 min in 10%H_2-N_2 atmosphere. O_2=0.027%, C=0.37%.

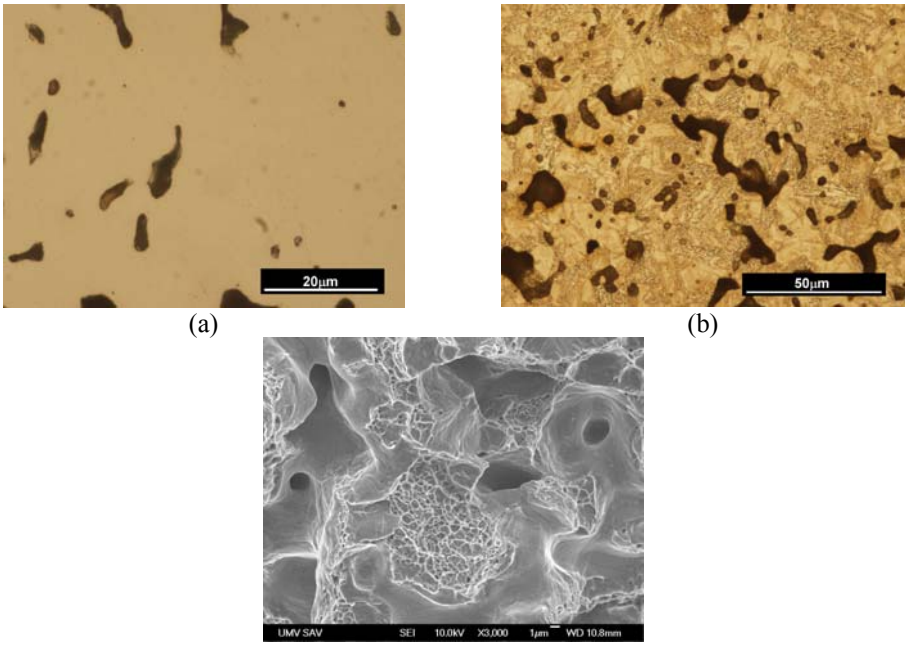

(a) (b)

(c)

Fig.5. Microstructure and fracture surface of the Fe-3Cr-0.5Mo-0.5C alloy with a density of 6.5 g·cm^{-3}, sintered at 1200°C for 30 min in 10%H_2-N_2 atmosphere. O_2=0.025%, C=0.36%.

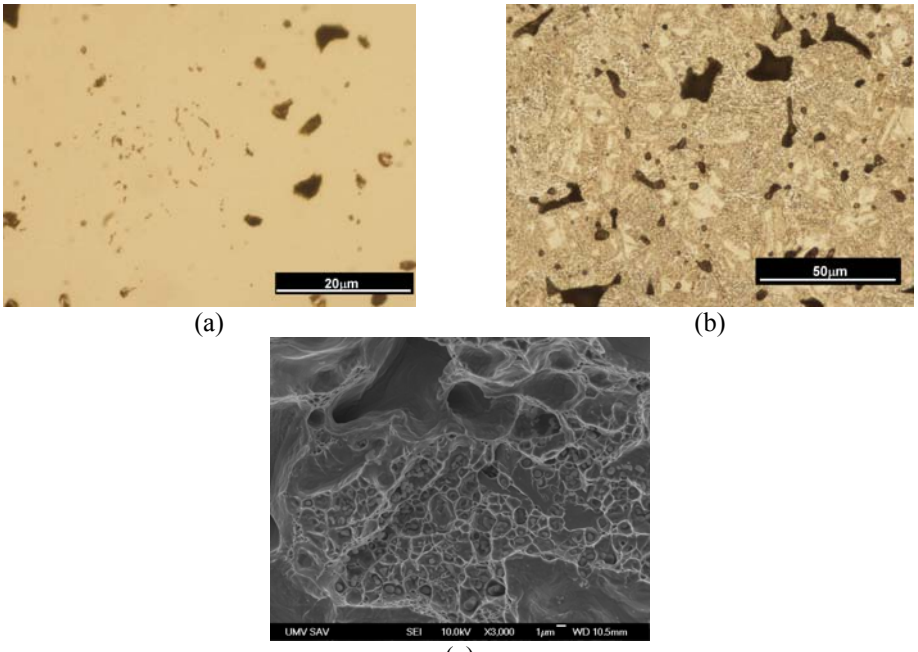

(a) (b)

(c)

Fig.6. Microstructure and fracture surface of the Fe-3Cr-0.5Mo-0.5C alloy with a density of 7.1 g·cm^{-3}, sintered at 1200°C for 30 min in 10%H_2-N_2 atmosphere. O_2=0.068%, C=0.39%.

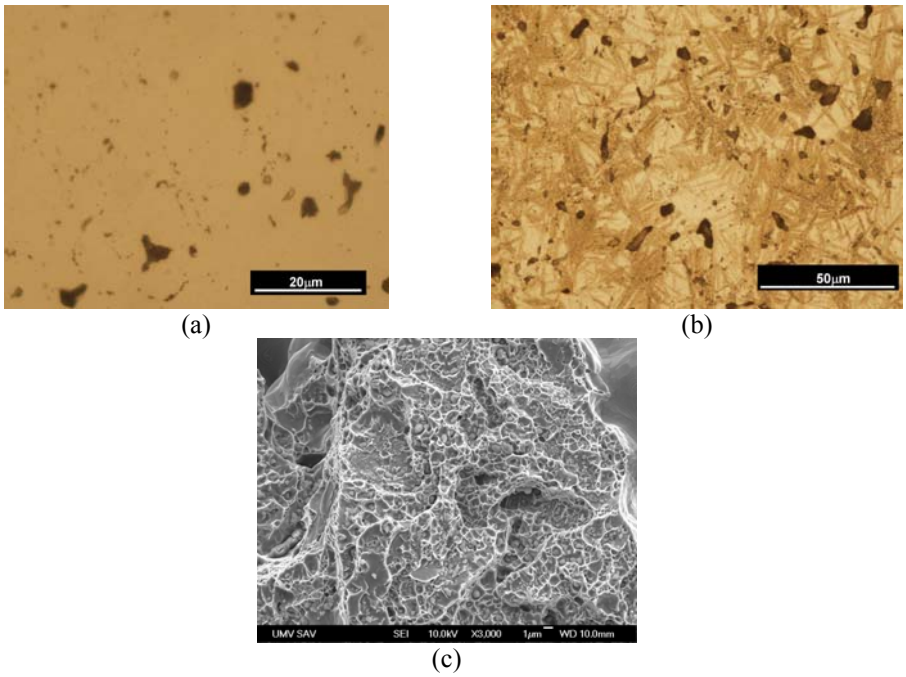

(a) (b)

(c)

Fig.7. Microstructure and fracture surface of the Fe-3Cr-0.5Mo-0.5C alloy with a density of 7.4 g·cm^{-3}, sintered at 1200°C for 30 min in 10%H_2-N_2 atmosphere. O_2=0.151%, C=0.41%.

Figures 5-7 show the effect of density on oxide purity of the material sintered at 1200°C. As a result of the higher oxygen content in the material with densities of 7.1 and 7.4 g·cm^{-3}, presence of oxide particles, distributed in the form of discontinuous networks located along grain boundaries and in the areas of the original particle surfaces, Figs.6a, 7a, is observed .

The failure in bainitic structure, Figs.5b-7b, is ductile with shallow dimples, Figs.5c-7c, but with significantly greater incidence of large shallow dimples in the case of density of 7.4 g·cm^{-3}. It is obvious that they are initiated by oxide particles or oxide particle clusters, Fig.7c. On the fracture surface was also observed local occurrence of intergranular fracture facets.

Semiquantitative EDX analysis of the oxide particles in shallow dimples showed that these are Cr-Mn-Si oxides of spinel-type, with ratio Cr:Mn close to 2:1 (~25 wt.% Cr, ~13 wt.% Mn, 0.20-0.25 wt.% Si, ~19 wt.% O_2). Such a relatively large residual oxidic contamination (0.151% O_2) of the material of density of 7.4 g·cm^{-3} caused a decrease of the fracture strength, down to 612 MPa.

Effect of heating and cooling rates

In order to study the effect of heating and cooling rates on final O_2 content, Table 2, two different heating and cooling rates, 10°C/min and 50°C/min, were applied. At higher heating and slower cooling rates, a tendency of increasing oxygen content is evident. In contrast, the combination of slower heating and faster cooling rate proved to be most favourable. It seems that various combinations of heating and cooling rates have no significant effect on the carbon content.

Tab.2. The effect of heating and cooling rates on the contents of O_2 and C and fracture strength.

Density [g·cm^{-3}]	Heat./Cool. rate [°C/min/ °C/min]	Sintering temperature [°C]	O_2 [%]	C [%]	R_{FR} [MPa]
6.5	10/10	1120	0.114	0.41	466
		1200	0.114	0.41	538
	50/10	1120	0.117	0.41	552
	10/50	1120	0.098	0.42	640
		1200	0.025	0.36	838
	50/50	1120	0.110	0.42	562
6.8	10/10	1120	0.118	0.41	566
		1200	0.076	0.35	725
	50/10	1120	0.120	0.41	620
	10/50	1120	0.097	0.42	754
		1200	0.027	0.37	929
	50/50	1120	0.108	0.42	945
7.1	10/10	1120	0.142	0.42	719
		1200	0.088	0.38	894
	50/10	1120	0.145	0.43	720
	10/50	1120	0.133	0.43	929
		1200	0.068	0.39	966
	50/50	1120	0.136	0.42	889

Effect of atmosphere purity

Two 10%H_2-N_2 sintering atmospheres of purity 5.0 and 6.0 with O_2 content of 2.0 vpm and 0.5 vpm were used. The compacts with densities of 6.5, 6.8, 7.1 g·cm^{-3} were sintered at 1120°C for 30 min with two different cooling rates: 10 and 50°C/min. No significant differences in processing gas composition were observed for both atmospheres and cooling rates used. However, the data in Table 3 indicate that lower O_2 content in the atmosphere of purity 6.0 may shift the thermodynamic balance in micro-climates towards reducing conditions. It is seen that reduction processes are controlled by both density and cooling rate, even for sintering in atmosphere of purity 6.0. The atmosphere purity does not have a significant effect on the final C-content, which ranges from 0.41-0.43%. However, the positive effect of atmosphere purity 6.0 and higher cooling rate resulted in higher fracture strength values.

Tab.3. O_2 and C contents and R_{FR} in relation to density, atmosphere purity and cooling rate, Astaloy CrM+0.5%C, 1120°C for 30 min.

Density [g·cm^{-3}]	Atmosphere purity	Cool. rate [°C/min]	O_2 [%]	C [%]	R_{FR} [MPa]
6.5	6.0	50	0.070	0.425	680
		10	0.095	0.41	559
	5.0	50	0.098	0.42	640
		10	0.114	0.41	466
6.8	6.0	50	0.090	0.43	788
		10	0.100	0.41	642
	5.0	50	0.097	0.42	754
		10	0.118	0.41	566

Density [g·cm^{-3}]	Atmosphere purity	Cool. rate [°C/min]	O_2 [%]	C [%]	R_{FR} [MPa]
7.1	6.0	50	0.125	0.43	948
		10	0.142	0.42	801
	5.0	50	0.133	0.43	929
		10	0.142	0.42	729

Sintering in N_2 atmosphere

Astaloy CrM+0.5% compacts with densities 6.5, 6.8, 7.1 g·cm^{-3} were sintered at 1120 and 1200°C for 30 min in N_2 atmosphere with a dew point of ~ -68°C after drying by liquid nitrogen. Heating and cooling rates were 10 and 50°C/min. Analyzing the profiles of H_2O, CO_2, CO contents in the processing gas, some differences between sintering in reducing, Fig.2, and inert, Fig.8, atmosphere, were identified. The amount of H_2O was significantly lower for the inert atmosphere. The peak at ~470°C, characteristic of reduction of Fe oxides by H_2, was not registered. The peak linked with CO_2 and H_2 reaction at ~1100°C was not identified as well. Small peaks on the CO curve at 400-600°C (graphite oxidation) were recorded. The peaks at ~800°C linked with reduction of Fe oxides by C were identified. With increasing density, the sharpness of peaks decreases, with a tendency to shift to higher temperatures. For density of 6.5 g·cm^{-3}, Fig.8a, there exists a small peak at 1112°C, linked to the reduction of surface Cr oxides and oxides from inner pores. When compared with sintering in H_2 containing atmosphere, Fig.2a, this peak is less pronounced; and at densities of 6.8 and 7.1 g·cm^{-3} it does not appear, Fig.8b. The peak at 1200°C, associated with carbothermic reduction of internal oxides and stable spinel Cr-Mn oxides, was recorded.

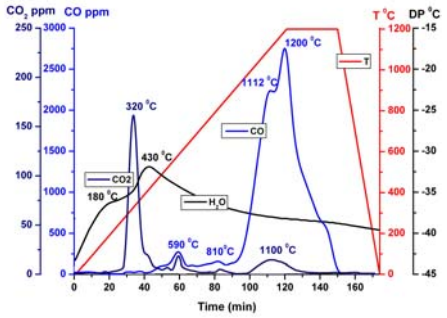

(a) 6.5 g·cm^{-3}

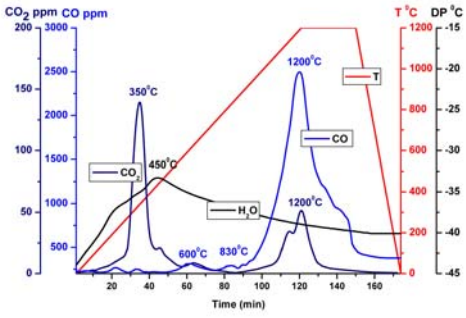

(b) 7.1 g·cm^{-3}

Fig.8. Records of processing gas composition during the sintering at 1200°C of Astaloy CrM + 0.5% C compacts with the density of 6.5 and 7.1 g·cm^{-3}, respectively in N_2 atmosphere.

Tab.4. O_2 and C contents and fracture strength resulting from sintering in N_2 atmosphere, Ast CrM + 0.5% C.

Density [g·cm^{-3}]	Sintering temperature [°C]	O_2 [%]	C [%]	R_{FR} [Mpa]
6.5	1120	0.125	0.410	537
	1200	0.044	0.360	803
6.8	1120	0.122	0.415	700
	1200	0.041	0.366	880
7.1	1120	0.136	0.430	815
	1200	0.093	0.380	943

Sintering in a graphite container

Astaloy CrM+0.5%C compacts of density 6.8 g·cm^{-3} were sintered at 1120°C for 30 min in a graphite container in N_2 atmosphere of purity 5.0. From the data in Table 5 it is evident, that a decrease in O_2 content by ~ 47% is achieved, which is still slightly lower when compared to sintering in H_2 containing atmosphere. At the same time the carbon content is slightly increased. The fracture strength is slightly lower when compared to sintering in H_2 containing atmosphere.

Tab.5. O_2 and C contents and R_{FR} using graphite container (N_2) and steel container (N_2 and 10%H_2-N_2).

Sintering condition	O_2 [%]	C [%]	R_{FR} [MPa]
Graphite container/N_2	0.105	0.44	721
Stainless steel container/N_2	0.122	0.42	700
Stainless steel container/10%H_2-N_2	0.097	0.42	754

Effect of carbon content

The compacts of Astaloy CrM+0.5, 0.6, 0.8%C with density of 6.8 g·cm^{-3} were sintered at 1120 and 1200°C for 30 min in 10%H_2-N_2 atmosphere of purity 5.0 and a dew point of ~ -68°C. Analyzing the profiles of H_2O, CO_2 and CO contents in the processing gas, it was found that the C content is particularly reflected in the temperature of the CO peaks, Table 6.

Tab.6. Characteristic temperatures of H_2O, CO and CO_2 peaks for graphite contents of 0.5, 0.6, 0.8%.

	H_2O			CO_2	CO			
peak	1	2	3	1	1	2	3	4
CrM+0.5C	180°C	470°C	1075°C	320°C	500°C	820°C	1120°C	1200°C
CrM+0.6C	182°C	470°C	1080°C	320°C	500°C	810°C	1100°C	1200°C
CrM+0.8C	170°C	470°C	1105°C	320°C	490°C	780°C	1074°C	1200°C

The first CO peak, related to reduction of Fe oxides with graphite in Fe/C contacts, was recorded at 820°C for 0.5% C, for 0.6% C it shifted to 810°C and to 780°C for 0.8% C, Fig.9. Second CO peak, associated with the carbothermal reduction of stable surface oxides and Fe oxides from the inner pores, was recorded at 1120°C for 0.5% C, for 0.6%C it is shifted to 1100°C and for 0.8% C to 1074°C. The temperature of H_2O peaks shows minimal

differences in relation to carbon content. The CO_2 peaks seem to be identical for alloys with different carbon additions.

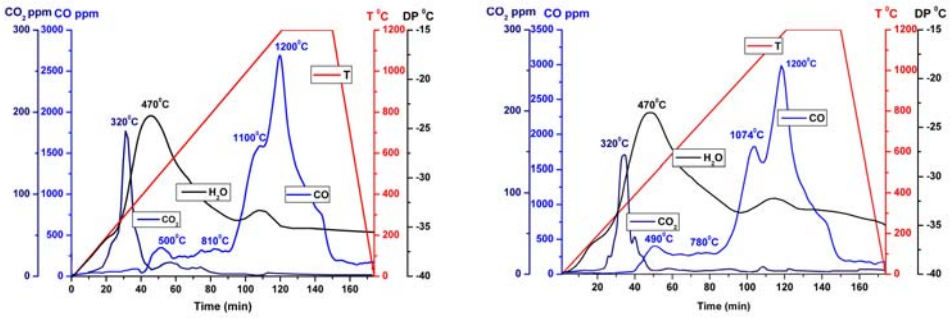

(a) (b)

Fig.9. Records of processing gas composition during the sintering of Astaloy CrM + 0.6 and 0.8% C compacts at 1200°C.

Data in Table 7 show that a higher amount of graphite addition leads to a decrease of O_2 content by 44-51% at 1120°C and by 83-86% at 1200°C. At the same time, the carbon content decreases by 16% for sintering at 1120°C and by 30% at 1200°C.

Tab.7. O_2 and C contents in relation to graphite addition, density of 6.8 g·cm^{-3}.

Graphite addition [%]	Temperature [°C]	O_2 [%]	C [%]	R_{FR} [MPa]
0.0	1200	0.161	-	128
0.5	1120	0.097	0.42	754
	1200	0.039	0.34	945
0.6	1120	0.110	0.50	690
	1200	0.034	0.42	847
0.8	1120	0.110	0.68	249
	1200	0.027	0.56	405

A significant decreasing R_{FR} values is a consequence of high carbon content resulting in the formation of a cementitic film at grain boundaries, clearly seen in Fig.10a, where the microstructure is of sintered material with carbon content (as sintered) of 0.56%. Figure 10b shows the presence of mixed intergranular and cleavage failure of material with carbon content of 0.56% sintered at 1200 C. It should be noted that the eutectoid point in the Fe-3Cr-C system is ~0.35% C at 786°C. Decrease in strength properties of sintered steels based on Astaloy CrM powder with a carbon content of ~0.45% was also confirmed by Dlapka [28].

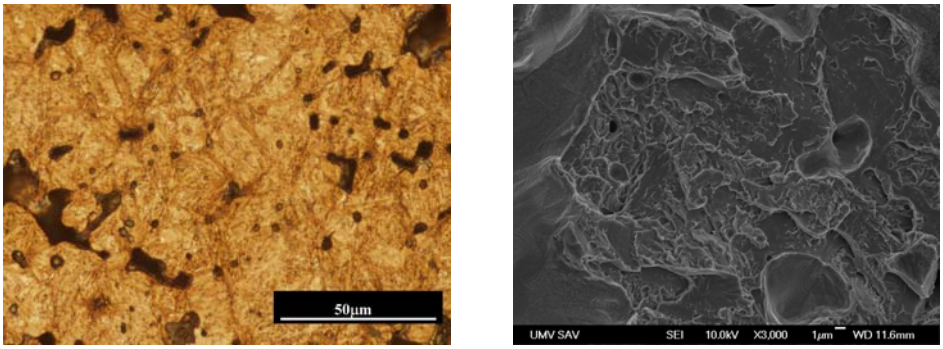

(a) (b)

Fig.10. Microstructure and fracture surface of the Fe-3Cr-0.5Mo alloy with density of 6.8 g.cm^{-3} and carbon content of 0.56% after sintering at 1200°C for 30 min in 10%H_2-N_2 atmosphere.

CONCLUSIONS

Information obtained regarding O_2 contents achieved and the corresponding fracture strength values for the processing conditions used are summarized in Figs.11,12.

Decrease in the oxygen content of more than 80% (83-87%), thus 0.025-0.034%O_2, was achieved for density of 6.5 and 6.8 g·cm^{-3} by sintering at 1200°C in both atmospheres, 10%H_2+N_2 (5.0) and N_2, at a cooling rate of 50°C/min.

Decrease in O_2 content by 50-75%, thus 0.05-0.099% O_2, was achieved for densities 6.5 and 6.8 g·cm^{-3} by sintering at 1120°C in an atmosphere of 10%H_2-N_2 (5.0 and 6.0) and cooling at 50°C/min. If the density of 7.1 g·cm^{-3} is needed, the temperature of 1200°C and the atmosphere of 10%H_2-N_2 (5.0), satisfy both the cooling rates (10 and 50°C/min).

Decrease in the oxygen content by 37.5-50%, thus 0.10-0.123% O_2, may be achieved for densities 6.5-6.8 g·cm^{-3} by sintering at 1120°C in both atmospheres, 10%H_2-N_2 (5.0) and N_2, at a cooling rate of 10°C/min.

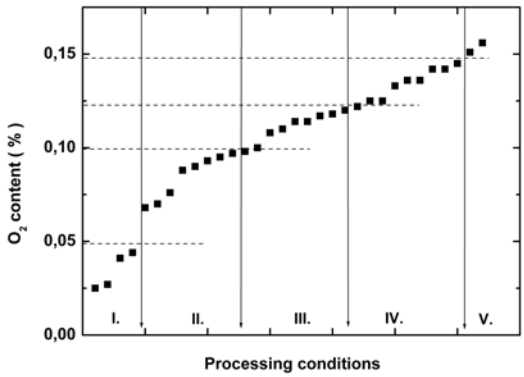

Fig.11. The oxygen content, depending on the experimental conditions. I - 1200-6.5, 6.8, H_2-N_2 (5.0), N_2, 50 = 1200 - temperature, 6.5 density, H_2-N_2 type of atmosphere,5.0 atmosphere purity, 50 - cooling rate; II - 1120- 6.5,6.8, H_2-N_2 (5.0, 6.0), 50; 1200-7.1, H_2-N_2, (5.0) 50, III - 1120- 6.5, 6.8, H_2-N_2 (5.0), N_2, 10, IV - 1120-7.1, H_2-N_2 (5.0), 10, 50, V - 1120, 1200-7.4, H_2-N_2 (5.0), 50.

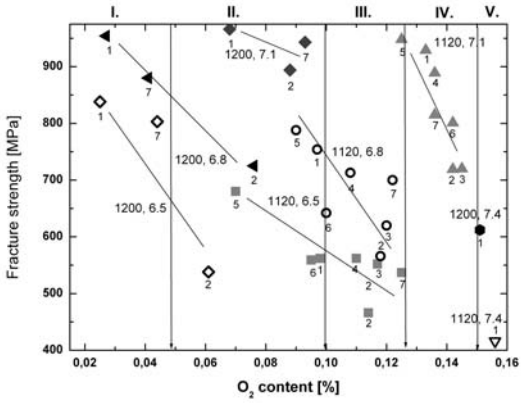

Fig.12. Fracture strength vs. oxygen content, depending of processing condition. 1 - 10/50 (5.0, H_2-N_2) = 10 - heating rate/50 - cooling rate,5.0 - atmosphere purity, H_2-N_2 - type of atmosphere; 2 - 10/10 (5.0, H_2-N_2), 3 - 50/10 (5.0, H_2-N_2), 4 - 0/50 (5.0, H_2-N_2), 5 - 10/50 (6.0, H_2-N_2), 6 - 10/10 (6.0, H_2-N_2), 7 - 10/50 (5.0, N_2).

Decrease in the oxygen content by 25-37.5%, thus 0.123-0.148% O_2, was achieved at a density of 7.1 g·cm^{-3} by sintering at 1120°C in both atmospheres, 10%H_2-N_2 (5.0) and N_2, and both cooling rates. The higher O_2 content corresponds to a lower cooling rate.

In the case of high density of 7.4 g·cm^{-3}, a decrease in the oxygen content was less than 25% for all conditions used. It should be noted that such a result is assumed to be connected with the massive oxide transformation from the iron-based to more chromium-based oxides during annealing before re-pressing. Additionally, such high-density results in pore closure inside the compact, meaning that there is no/limited interaction with the processing atmosphere. Therefore poor resulting microclimate inside the compact leads to unsatisfactory surface oxide reduction and therefore poor mechanical properties.

In terms of relation between the fracture strength and O_2 content, it is obvious that strength properties, in addition to the oxygen content, are controlled by density and microstructure. The higher O_2 content causes a weakening of interfaces with residual oxides.

Acknowledgement

Authors are grateful for financial support Slovak National Grant Agency (project VEGA 2/0153/12).

REFERENCES

[1] Berg, S., Maroli, B. In: Advances in PM and Part. Mater. Part 8. Princeton, NJ : MPIF, 2002, p. 1
[2] Bergman, O. In: EURO PM 2003. Vol. 1. Shrewsbury, UK : EPMA, 2003, p. 317
[3] Carlsson, M., Johansson, P., Frykholm, R.: Int. J. of Powder Metall., vol. 40, 2004, no. 5, p. 15
[4] Karlsson, H., Nyborg, L., Berg, S.: Powder Metall., vol. 48, 2005, no. 1, p. 51
[5] Engström, U., Millingan, D., Klekovkin, A. In: Advances in PM and Particulate Materials. Vol. 1., Part 7. Princeton, N.J. : MPIF, 2006, p. 1
[6] Bergman, O., Lindquist, B., Bengtsson, S.: Mater.Sci.Forum, vol. 534-536, 2007, p. 545
[7] Engström, U., Frykholm, R., Millingan, D., Warzel, R. In: Advances in Powder

Metallurgy and Particulate Materials. Part 10. Princeton, N.J. : MPIF, 2008, p. 10
[8] Karlsson, H.: PhD Thesis. Goteborg : Chalmers University of Technology, 2005
[9] Chasoglou, D., Hryha, E., Nyborg, L.: Powder Metallurgy Progress, vol. 9, 2009, no. 3, p. 41
[10] Ortiz, P., Castro, F.: Powder Metallurgy, vol. 47, 2004, no. 3, p. 291
[11] Mitchell, SC., Cias, A.: Powder Metallurgy Progress, vol. 4, 2004, no. 3, p.132
[12] Hryha, E., Gierl, C., Nyborg, L., Danninger, H., Dudrová, E.: Appl. Surface Science, vol. 256, 2010, p. 3946
[13] Hryha, E., Nyborg, L., Gierl, C., Danninger, H. In: Proc.World Congr. PM 2010. Vol. 1. Florence, Italy, 2010, p. 25
[14] Hryha, E., Dudrová, E., Nyborg, L.: J. of Materials Processing Technology, vol. 212, 2012, p. 977
[15] Hryha, E., Čajková, L., Dudrová, E.: Powder Metallurgy Progress, vol. 7, 2008, no. 4, p. 181
[16] Danninger, H., Xu, C., Lindquist, B.: Materials Science Forum, vol. 534-536, 2007, p. 577
[17] Danninger, H., Gierl, C., Kremel, S., Leitner, G., Jaenicke-Roessler, K.: P/M Science and Technology Briefs, vol. 6, 2004, no. 3, p. 10
[18] Danninger, H., Gierl, C., Kremel, S., Leitner, G., Jaenicke-Roessler, K., Yu, Y.: Powder Metallurgy Progress, vol. 2, 2002, no. 3, p. 125
[19] Danninger, H., Gierl, C.: Science of Sintering, vol. 40, 2008, p. 33
[20] Danninger, H., Xu, C. In: Proc. EURO PM 2003. Part:.Low Alloyed Steels, p. 269
[21] Ortiz, P., Castro, F.: Materials Science Forum, vol. 426-432, 2003, p. 4337
[22] Hryha, E., Nyborg, L. In: Proc. of the World Congress PM 2010. Vol. 2. Florence, Italy, 2010, p. 267
[23] Chasoglou, D., Hryha, E., Nyborg, L. In: Proc. World Congress PM 2010. Vol. 2. Florence, Italy, 2010, p. 3
[24] Hryha, E., Dudrová, E. In: Application of Thermodynamics to Biological and Materials Science. Ed. M. Tadashi. Vol. 22. Rijeka : InTech, p. 573
[25] Čiripová, L., Hryha, E., Dudrová, E., Výrostková, A.: Materials and Design, vol. 35, 2012, p. 619
[26] Hryha, E.: PhD Thesis. Kosice : IMR SAS, 2007
[27] Hrubovčáková, M., Dudrová, E.: Powder Met. Progress, vol. 10, 2010, no. 2, p.71
[28] Dlapka, M.: PhD. Thesis. Vienna : TU, 2011
[29] Hrubovčáková, M., Dudrová, E., Harvanová, J.: Powder Met. Progress, vol. 11, 2011, no.1-2, p.115